SPACE TELESCOPE SCIENCE INSTITUTE
Operated for NASA by AURA

Instrument Science Report ACS 2011-02

Flux Calibration of the ACS CCD Cameras

II. Encircled Energy Correction

Ralph C. Bohlin

April 29, 2011

Abstract

In order to convert a point source flux calibration into a surface brightness calibration, the total response to a point source in an infinite aperture is required. In practice, infinite is defined as an aperture with a radius of 5″.5. However, aperture photometry for such a large radius is exquisitely sensitive to the measured sky background level. In order to minimize uncertainties, corrections from one arcsec to infinity (5″.5) are derived from averages over as many heavily exposed, isolated stellar images as possible. Calibrations, such as the change in sensitivity with time or flux calibrations from specific standard stars, utilize the low noise photometry for one arcsec radius; and the average correction to infinite aperture is used only as required. This ISR deals with the ACS encircled energy for one arcsec relative to infinity for the HRC and WFC.

1. Introduction

Absolute flux calibrations of quantitative astronomical data are normally derived from observations of standard candles, i.e. stars that have the best known absolute flux tabulations of their spectral energy distributions (SEDs). A standard reference aperture size is

established for which the extraction of the observed signal is most repeatable, i.e. photometric, over the instrumental lifetime. Since the flux standards are bright stars, a large aperture is chosen, which is a one arcsec radius for the ACS WFC and HRC channels. For crowded field photometry, smaller apertures are required; and aperture corrections must be derived relative to the fiducial one arcsec size. The smaller the extraction aperture, the greater the dependence of the encircled energy fraction on focus and variability of focus across the field of view.

Because standards of diffuse surface brightness are not well established around the sky, the calibration in physical units of specific intensity for diffuse objects must be derived from point sources and requires an estimate of the total signal from the standard star in an infinite aperture. For the Equations and details of the flux and specific intensity calibrations for filter photometry, see Bohlin, et al. (2011, hereafter B11). For the two ACS CCD channels, a radius of 5″.5 is chosen to approximate infinity (Sirianni et al. 2005, hereafter S05; Bohlin 2007, hereafter B07). A theoretical check on the assumption that 5″.5 contains all of the PSF is not possible with Tiny Tim, because the user manual states: "At short wavelengths, it may not be possible to compute a PSF larger than 7″. Generally, the models are not very good past a radius of ∼2″, due to the effects of scatter and high-frequency aberrations" (Krist and Hook 2004).

This ISR is the second (II) in a four part series that will culminate with a new flux calibration for the ACS CCD detectors. Based on the pixel level CTE correction technique of Anderson & Bedin (2010), ISR I (Bohlin & Anderson 2011) defined the CTE losses for observations of the bright standard stars with the WFC CCD. ISR III will deal with the sensitivity changes over time. Here, the aperture corrections for photometry in a one arcsec radius vs. an "infinite" (5″.5) radius are presented. The small Bohlin & Anderson CTE corrections are applied to the 1″ photometry; but all of the temporarily trapped charge is assumed to be re-emitted and captured in an aperture as large as our (5″.5) radius.

2. Analysis of the Hot Star Data

Following de Marchi et al. (2004), Bohlin & Gilliland (2004, BG), S05, and B07, a 5″.5 photometric aperture is defined to contain all the signal from a stellar point source. Sky backgrounds are defined in the annuli of 6-8″ for WFC and 5.6-6″.5 for HRC. Total stellar signals are required to define the diffuse-source surface-brightness calibration and to compare with predicted count rates from the component throughput measurements. Aperture photometry is computed with the IDL program apphot.pro (Landsman 2004 pers. comm.). The apphot.pro photometry is verified against IRAF results, and photometry from the crj

files plus pixel area maps is equivalent to photometry from the drz files. For the WFC observations of the bright star BD+17°4804 (BG), the *flt* files must be used because of saturation of the CCD in a few central pixels of the images. However, Gilliland (2004) demonstrated the linearity of such saturated data to 0.1%, as long as the A-to-D converter does not saturate, i.e. gain=2 is required. For the 2009 WFC observations of BD+17°4804, some of the exposure times were increased from 1 to 2s, which occasionally causes a few saturated pixels to fall outside the 1″ aperture. A limit of $\sim 7 \times 10^6$ electrons in an individual image corresponds to the onset of this excess saturation and is exceeded for the 2s exposures in F606W, F625W, and F814W, which cannot be used in this analysis.

Table 1 summarizes the number of valid measurements by star, camera, and filter. In addition to the $\sim 7 \times 10^6$ electron constraint, encircled energy (EE) measurements are excluded if the sub-array size is less than 1024x1024, if the star is more than 4″ for HRC or 8″.4 for WFC from the reference point, or if the sub-array lacks overscan data. The HRC reference point is the center of the detector, while for WFC the standard WFC1-1K sub-array is centered on chip 1 at (3583,1535). Individual EE values with large formal uncertainties are also excluded from the averages.

Average EE values for the ten bright standard stars are displayed in Figures 1 and 2 as a function of the filter pivot wavelength. The 3σ error-in-the-mean for the average of the four WDs plus the F, G, and K stars are shown as the error bars. Heavy black lines are the polynomial fits to these averages for the seven hotter stars, i.e. cubic for WFC and fourth order for HRC. The cool stars VB8 (M7), 2M0036+18 (L3.5), and 2M0559-14 (T5) are excluded because of the scattered red-light problem for the long wavelength filters, as discussed in §3. For the filters shortward of 7000Å, the fluxes for the cool stars drop steeply, so that the count rates are relatively low and the exposure times corresponding longer, which increases the effect of noise from cosmic-ray hits and hot pixels in the huge 5″.5 aperture. Thus, all photometry with less than 16,000 counts/s for WFC and 10,000 counts/s for HRC are excluded from the average EE correction and are not shown in Figures 1 or 2, except for 2M0036+18 and 2M0559-14 in the longest wavelength filters.

Because the stellar signal is about the same but the area of a 5″.5 aperture is 30 times the area of a standard 1″ aperture, the uncertainty in the 5″.5 photometry that is attributed to the uncertainty in the sky level is ∼30x larger for the 5″.5 aperture than for the 1″ aperture. Thus, the fitted polynomials smooth the effects of residual noise and define the correction for the total EE from radius=1 to radius=5″.5. The 5″.5 photometry is exquisitely sensitive to the measured background sky level; and only these averaged and smoothed results should be considered accurate at the $\lesssim$1% level. No error bars are shown for the narrow band filters, which are excluded from the fitted data. Narrow band observations are more uncertain

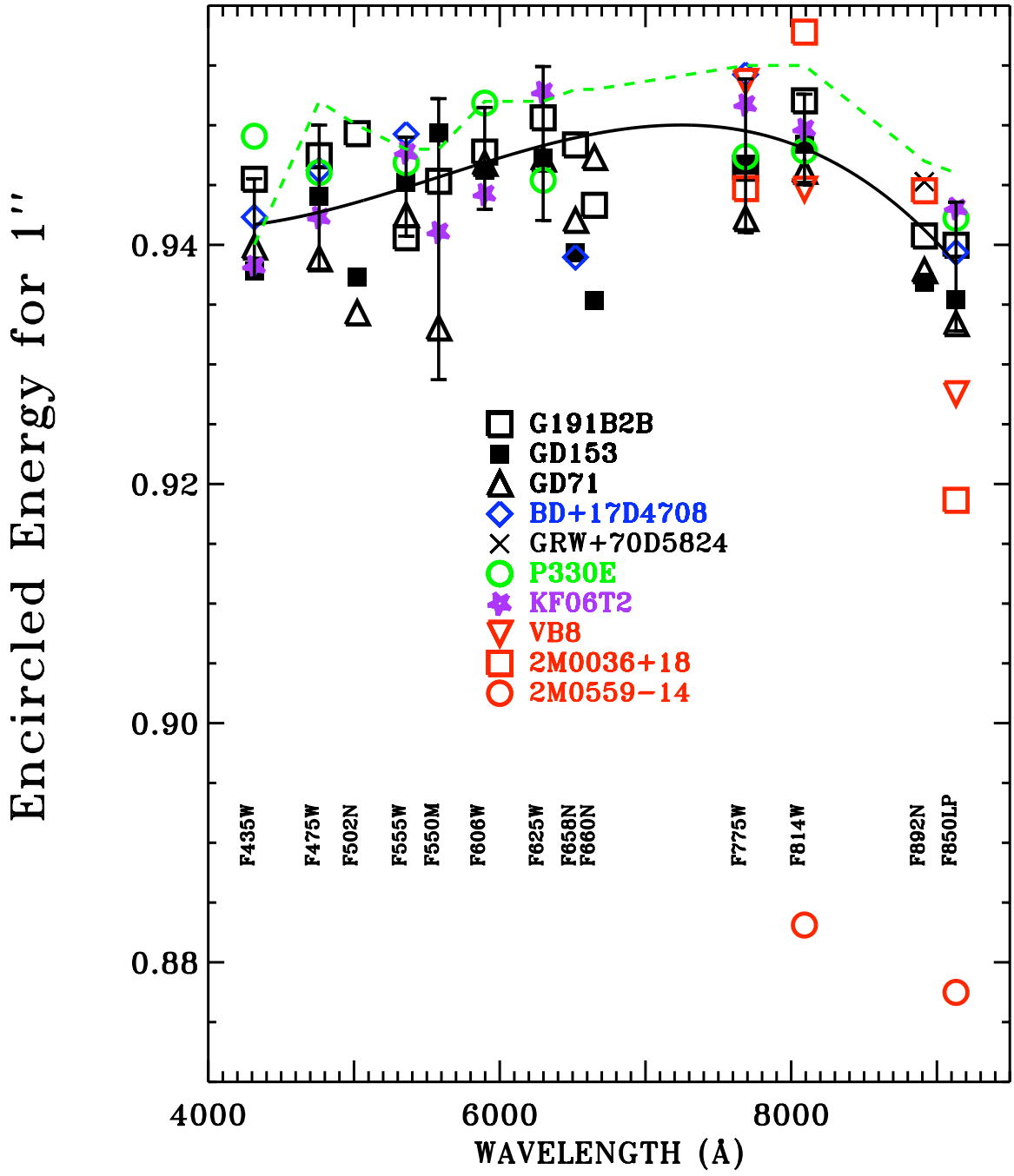

Fig. 1.— Encircled energy for WFC, i.e. fraction of signal in a one arcsec aperture relative to an "infinite" aperture of 5.5 arcsec radius. The solid black line is a polynomial fit to the averages of the EE from the WDs, the F star (BD+17°4708), the G star (P330E), and the K star (KF06T2). Error bars are $\pm 3\sigma$ error in the mean of these averages, but the averages are not shown to avoid congestion. The green dashed lines are the results of S05.

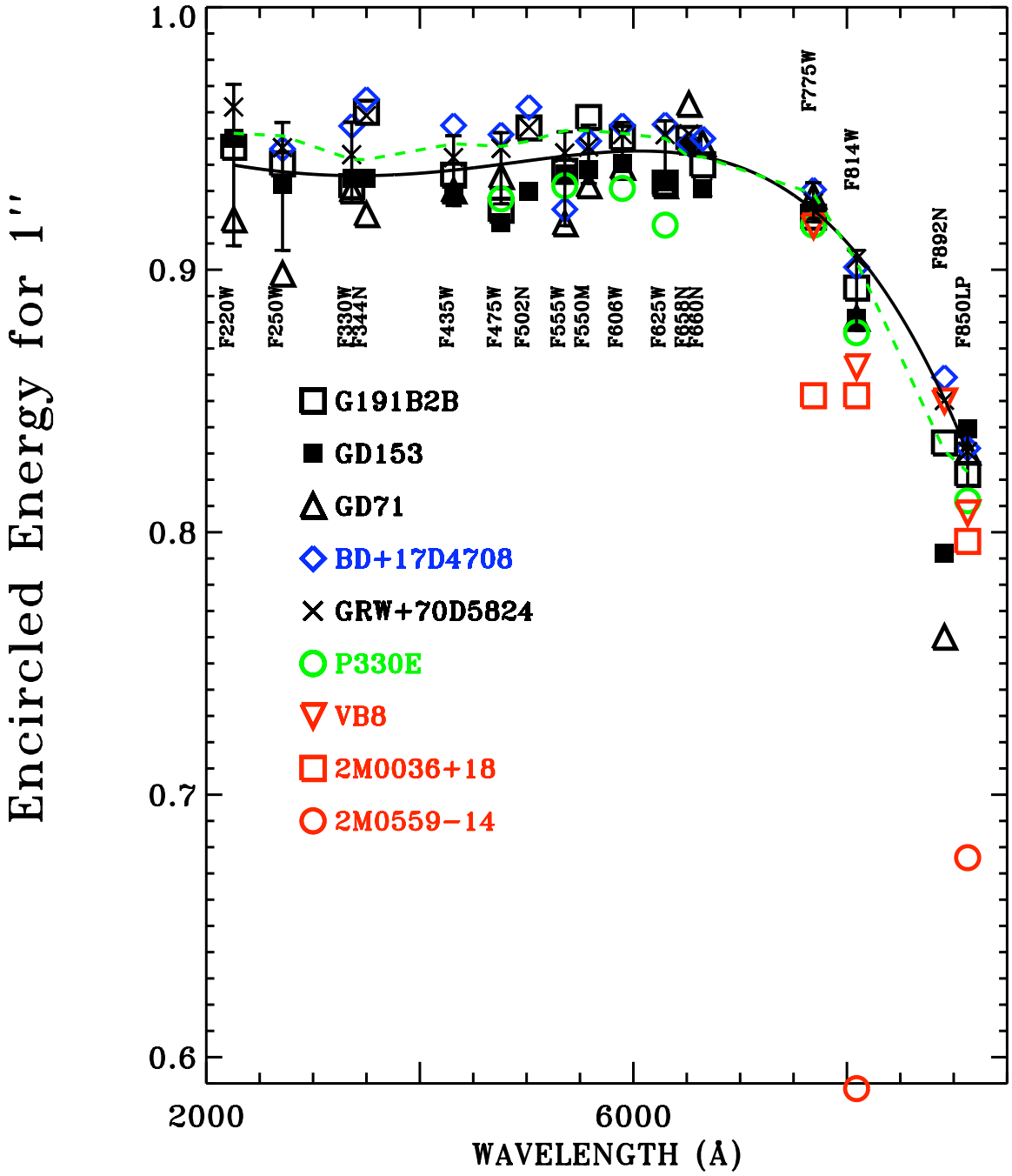

Fig. 2.— As in Figure 1 for HRC, except that there are no data for the K star (KF06T2).

Filter	G191B2B DA0	GD153 DA1	GD71 DA1	GRW+70°5824 DA3	BD+17°4804 sdF8	P330E G0V	KF06T2 K1.5III	VB8 M7	2M0036+18 L3.5	2M0559-14 T5
WFC										
F435W	3	3	3	...	2	1	2	...	...	...
F475W	2	3	2	...	2	1	2	...	...	...
F502N	1	1	1	...	...	...	...	...	...	...
F550M	1	1	2	...	...	...	2	...	...	...
F555W	3	4	3	...	2	2	2	...	...	...
F606W	3	4	2	...	...	2	2	...	...	...
F625W	3	4	3	...	...	2	2	...	...	...
F658N	2	1	2	...	1	...	...	...	...	...
F660N	1	1	1	...	...	...	...	...	...	...
F775W	3	4	3	...	2	2	2	3	2	...
F814W	3	4	3	...	...	2	2	3	1	2
F892N	2	2	2	5	...	...	...	...	1	...
F850LP	3	4	3	...	2	2	2	3	1	2
HRC										
F220W	3	2	3	1	...	...	...	...	...	...
F250W	3	2	3	4	1	...	...	...	...	...
F330W	3	2	3	6	4	...	...	...	...	...
F344N	1	1	2	4	1	...	...	...	...	...
F435W	3	2	2	4	1	...	...	...	...	...
F475W	3	2	2	4	6	1	...	...	...	...
F502N	1	1	...	4	1	...	...	...	...	...
F550M	1	1	2	4	1	...	...	...	...	...
F555W	2	2	2	4	1	1	...	...	...	...
F606W	3	2	1	4	1	1	...	...	...	...
F625W	2	2	1	4	6	1	...	...	...	...
F658N	1	1	1	4	1	...	...	...	...	...
F660N	1	1	1	4	1	...	...	...	...	...
F775W	3	2	2	4	6	1	...	3	1	...
F814W	2	2	2	4	1	1	...	3	2	1
F892N	2	1	1	4	1	...	...	1	...	...
F850LP	2	2	2	4	6	1	...	3	2	1

Table 1: *Number of observations that are used to define the EE for each star and filter.*

because spectral lines in the standard star SEDs are not perfectly defined, because tiny errors in the bandpass functions are magnified by sharp spectral features, and because the longer exposures increase the cosmic-ray noise. Green dashed lines are the EE results from S05. Table 2 summarizes the results from the fitted curves, where the values are smaller than tabulated in B07 by as much as 0.014 (for HRC F330W) because of better bias subtraction. The new WFC values range from the same value as B07 for F435W to 0.004 higher for F775W. Typical formal 1σ uncertainties on the fitted values in Table 2 are 0.003 for WFC and 0.007 for HRC.

The new results differ by 0.02, at most, from S05 as shown in Figures 1 and 2, despite the mostly different data sets used to derive the EE. S05 used only GD71 and GRW+70°5824; and those early data are now excluded because of the lack of any overscan on the WFC1 subarrays. The new WFC EEs are lower than the S05 values, probably because S05 included

Filter	WFC	HRC
F220W	...	0.940
F250W	...	0.937
F330W	...	0.936
F344N	...	0.936
F435W	0.942	0.938
F475W	0.943	0.940
F502N	0.944	0.942
F555W	0.945	0.943
F550M	0.946	0.944
F606W	0.947	0.945
F625W	0.948	0.945
F658N	0.949	0.944
F660N	0.949	0.943
F775W	0.950	0.923
F814W	0.948	0.906
F892N	0.941	0.851
F850LP	0.938	0.830

Table 2: *One Arcsec Encircled Energy Fractions for Hot Stars*

the chip 2 data for GD71, which is systematically higher by 1-4%. These chip 2 data are from small 512x512 sub-arrays with no overscan, where the 8″ outer background radius often falls outside the sub-array.

The source independent $photflam \equiv P_\lambda$ flux calibration constant in the ACS header keyword defines the photon weighted mean flux $\langle F_\lambda \rangle$ per B11 as

$$\langle F_\lambda \rangle = P_\lambda N_e \ , \tag{1}$$

where N_e is the total response in an infinite aperture in electrons/s and λ represents wavelength. In practice, the total response N_e in the 5″.5 infinite aperture cannot be measured in most ACS CCD science images, so that for the best precision, the aperture corrections for each image should be relative to N_1, the electrons/s in the one-arcsec, primary-reference aperture. Mean fluxes are then defined as

$$\langle F_\lambda \rangle = P_\lambda N_1 / C_1 \ , \tag{2}$$

where C_1 is from Table 2; and N_1/C_1 is our definition of N_e.

3. Analysis of the Cool Star Data

Red stars of spectral type M and later have a "red halo" and show significantly lower EE, because long wavelength photons scatter more in the CCD substrates, especially for HRC, which lacks the special anti-scattering layer incorporated into the WFC CCDs. Figures 1 and 2 shows these red star EE values as red data points; and Figure 3 compares their SEDs to the "hot stars". Digital versions of these SEDs are available from the CALSPEC database[1]. S05 provide their tables 6-7, which define the EE parameterized by the effective wavelengths, which are not constant for a filter but increase as the peak of the stellar flux distributions move to longer wavelengths. The S05 values for the effective wavelengths are wrong due to an error in the old Synphot software used by S05; however, those incorrect values must still be used to interpolate in the S05 tables 6-7. Table 3 includes these S05 EE values to compare with the Table 2 values for hotter stars and with the new values that are derived directly from the measurements.

The sparse EE measures often have low count rates for many of the red points, so that the EE values have larger uncertainties than the 1σ values 0.003 for WFC and 0.007 for HRC quoted above for the ensemble hotter-star values in Table 2 that are copied to column two of Table 3. Only VB8 in the three longwave broadband filters has count rates above the limits for the hotter stars, i.e. 16,000 counts/s for WFC and 10,000 counts/s for HRC. For WFC, the only discrepancy with S05 is for 2M0559-14 in the F814W filter. There are two direct measures of this EE, 0.870 and 0.895, both of which are below the S05 value of 0.94. Similarly, the two EE values for 2M0559-14 in the F850LP are 0.863 and 0.891. With a formal 3σ uncertainty of $\sim$0.04, the 0.88 values for the coolest star 2M0559-14 in column (7) make a good case for a small loss of scattered red light, especially for F850LP, where the independent S05 value provides confirmation. The directly measured values for WFC F814W for 2M0559-14 and for all three red stars in F850LP in Table 3 are recommended, whereas the Table 2 values are adopted for all other WFC cases; although, a better guess for the unmeasured F892N for SEDs similar to 2M0559-14 might be 0.88.

Judging from the differences between the "New" value and the S05 values for HRC, systematic uncertainties may be 3% for VB8 and 6% for 2M0036+18, while the 2M0559-14 uncertainties may be 10-20%. The S05 figure 8 shows a value for VB8 in HRC F850LP closer to the "New" value than to their interpolated value of 0.78. The biggest discrepancy between the new measurements and S05 for HRC is 2M0559-14 in the F814W filter. In this case, the single measurement has a formal uncertainty of 0.31. None of the other new measurements differ significantly from S05. Thus, all of the smoothly parameterized EE of S05 in Table

[1]http://www.stsci.edu/hst/observatory/cdbs/calspec.html

3 are adopted for HRC, while the Table 2 HRC values are recommended for the red stars observations in filters shortward of F775W.

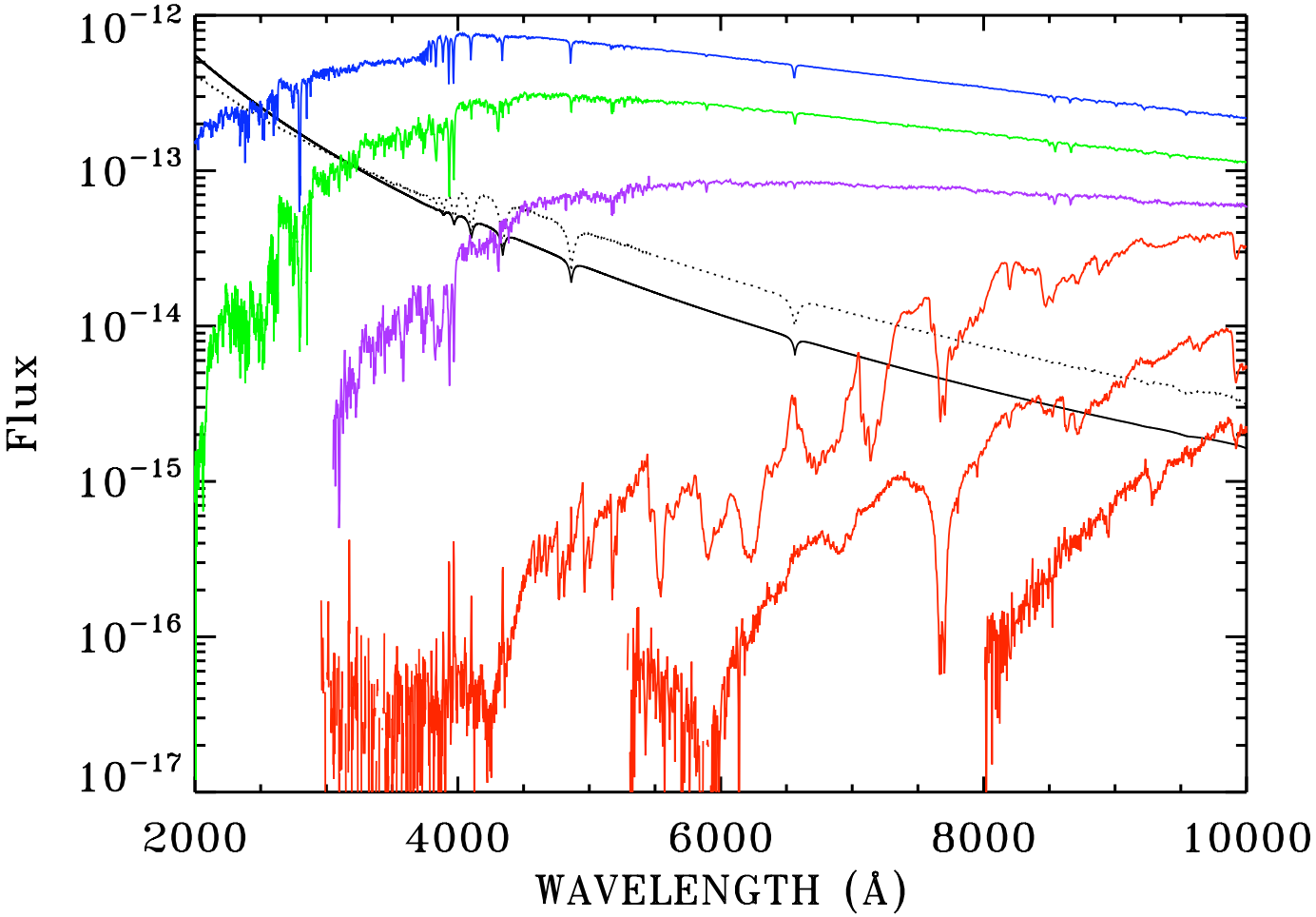

Fig. 3.— SEDs of stars used to measure the EE with the same color coding as for Figure 1. The dotted black line is GRW+70°5824, while the prime WD GD153 is the solid black line. The red curves in order of bright to faint are VB8, 2M0036+18, and 2M0559-14. For clarity, the SEDs for P330E, KF06T2, 2M0036+18, and 2M0559-14 are scaled up by factors of 12, 8, 4, and 5, respectively.

In summary, for flux distributions similar to the red curves in Figure 3, the use of the *photflam* header keyword for hot stars must be modified to estimate the mean flux in the bandpass:

$$\langle F_\lambda \rangle = P_\lambda N_1 / C_* \ , \tag{3}$$

where C_* are the EE values flagged in Table 3.

Filter	Hot-Star	VB8 (M7)		2M0036(L3.5)		2M0559(T6.5)	
		New	S05	New	S05	New	S05
(1)	(2)	(3)	(4)	(5)	(6)	(7)	(8)
WFC							
F814W	0.948	0.945	0.95	0.96	0.95	0.88*	0.94
F892N	0.941	...	0.94	0.94	0.94	...	0.94
F850LP	0.938	0.93*	0.93	0.92*	0.92	0.88*	0.88
HRC							
F775W	0.923	0.92	0.91*	0.85	0.91*	...	0.90*
F814W	0.906	0.86	0.86*	0.85	0.85*	0.59	0.82*
F892N	0.851	0.85	0.84*	...	0.84*	...	0.84*
F850LP	0.830	0.81	0.78*	0.80	0.76*	0.68	0.66*

Table 3: *Encircled Energy for One Arcsec for Cool Stars. Use column (2) values, which are from Table 2, except for the values that are flagged with an asterisk.*

References

Anderson, J., & Bedin, L. R. 2010, PASP, **122**, 1035

Bohlin, R. C. 2007, Instrument Science Report, ACS 2007-06, (Baltimore:STScI) (B07)

Bohlin, R. C., & Anderson, J. 2011, Instrument Science Report, ACS 2011-01, (Baltimore:STScI)

Bohlin R. C., & Gilliland, R. L. 2004, AJ, 127, 3508 (BG)

Bohlin R. C., Gordon, K. D, Rieke, G. H., Ardila, D., Carey, S., Deustua, S., Engelbracht, C., Ferguson, H. C., Flanagan, K., Kalirai, J., Meixner, M., Noriega-Crespo, A., Su, K. Y. L., and Tremblay, P. E. 2011, AJ, 141, 173 (B11)

De Marchi, G., Sirianni, M., Gilliland, R., Bohlin, R., Pavlovsky, C., Jee, M., Mack, J., van der Marel, R., & Boffi, F. 2004, Instrument Science Report, ACS 2004-08, (Baltimore:STScI)

Gilliland, R. L., Bohlin, R. C., & Mack, J. 2006, Instrument Science Report, ACS 2006-06, (Baltimore:STScI)

Krist, J., & Hook, R. 2004, The Tiny Tim User's Guide, Version 6.3, http://www.stsci.edu/software/tinytim, p. 8

Sirianni, M., et al. 2005, PASP, 117, 1049S (S05)